MOLECULAR AND CELLULAR BIOLOGY, Dec. 2005, p. 10979–10988 Vol. 25, No. 24
0270-7306/05/$08.00+0 doi:10.1128/MCB.25.24.10979–10988.2005

Phospholipase C-δ1 and -δ3 Are Essential in the Trophoblast for Placental Development

Yoshikazu Nakamura,[1] Yoshio Hamada,[2] Takashi Fujiwara,[3] Hiroko Enomoto,[1] Takeshi Hiroe,[4] Satoshi Tanaka,[5] Masato Nose,[6] Masamichi Nakahara,[1] Nobuaki Yoshida,[7] Tadaomi Takenawa,[8] and Kiyoko Fukami[1]*

Laboratory of Genome and Biosignal, Tokyo University of Pharmacy and Life Science, 1432-1 Horinouchi, Hachioji, 192-0392 Tokyo, Japan[1]; Tissue and Cell Culture Laboratory, National Institute For Basic Biology, 38 Nishigonaka, Myodaiji, Okazaki, Aichi 444-8585, Japan[2]; Laboratory Animal Center, Ehime University School of Medicine, Shitsukawa, Shigenobu-cho, Onsen-gun, Ehime 791-0295, Japan[3]; Center for Experimental Animals, National Institute for Physiological Sciences, 38 Nishigonaka, Myodaiji, Okazaki 444-8585, Japan[4]; Laboratory of Cellular Biochemistry, Department of Animal Resource Sciences/Veterinary Medical Sciences, The University of Tokyo, Yayoi 1-1-1, Bukyo-ku, Tokyo 113-8657, Japan[5]; Department of Pathology, Ehime University School of Medicine, Shitsukawa, Shigenobu-cho, Onsen-gun, Ehime 791-0295, Japan[6]; Division of Gene Expression and Regulation, The Institute of Medical Science, University of Tokyo, 4-6-1 Shirokanedai, Minato-ku, Tokyo 108-8639, Japan[7]; and Department of Biochemistry, The Institute of Medical Science, University of Tokyo, 4-6-1 Shirokanedai, Minato-ku, Tokyo 108-8639, Japan[8]

Received 19 August 2005/Returned for modification 2 September 2005/Accepted 18 September 2005

Phosphoinositide-specific phospholipase C (PLC) is a key enzyme in phosphoinositide turnover and is involved in a variety of physiological functions. We analyzed *PLCδ1* knockout mice and found that PLCδ1 is required for the maintenance of skin homeostasis. However, there were no remarkable abnormalities except hair loss and runting in *PLCδ1* knockout mice, even though PLCδ1 is broadly distributed. Here, we report that mice lacking both *PLCδ1* and *PLCδ3* died at embryonic day 11.5 (E11.5) to E13.5. *PLCδ1*/*PLCδ3* double-knockout mice exhibited severe disruption of the normal labyrinth architecture in the placenta and decreased placental vascularization, as well as abnormal proliferation and apoptosis of trophoblasts in the labyrinth area. Furthermore, *PLCδ1*/*PLCδ3* double-knockout embryos supplied with a normal placenta by the tetraploid aggregation method survived beyond E14.5, clearly indicating that the embryonic lethality is caused by a defect in trophoblasts. On the basis of these results, we conclude that PLCδ1 and PLCδ3 are essential in trophoblasts for placental development.

Phosphoinositide-specific phospholipase C (PLC) hydrolyzes phosphatidylinositol 4,5-bisphosphate to generate two second messengers, diacylglycerol and inositol 1,4,5-trisphosphate. Diacylglycerol mediates the activation of protein kinase C, and inositol 1,4,5-trisphosphate releases calcium from intracellular stores (1, 19).

PLC can be categorized into six types, β, γ, δ, ε, ζ, and η, on the basis of sequence homology and activation mechanism (5, 13, 20, 21, 23, 24, 34). Each isozyme is composed of subtype-specific and conserved domains. All PLC isozymes contain catalytic X and Y domains, as well as various regulatory domains, including the C2 domain, EF-hand motif, and pleckstrin homology domain. Subtype-specific domains contribute to the specific regulatory mechanisms. These domains include the src homology domain in PLCγ (23) and the Ras-associating domain and Ras-GTPase exchange factor-like domain in PLCε (15, 29).

PLCδ types are evolutionarily conserved from lower to higher eukaryotes, and these isozymes are thought to be the primary forms expressed in mammals. Therefore, PLCδ is expected to have important and basic physiological functions. There are three PLCδ isozymes, PLCδ1, -δ3, and -δ4 (10). It has been suggested that PLCδ1 is involved in Alzheimer's disease (27) and essential hypertension (14, 35). Recently, we analyzed *PLCδ* knockout (KO) mice and found that PLCδ1 has an important role in skin homeostasis (18) and that PLCδ4 is involved in the acrosome reaction of sperm (6, 7). These results provide some clarification of the physiological functions of PLCδ1 and PLCδ4; however, the function of PLCδ3 remains unknown.

In the present study, to elucidate the physiological roles of PLCδ3, we analyzed *PLCδ3* KO mice. Thus far, *PLCδ3* KO mice have exhibited no obvious abnormalities. Because *PLCδ3* is most similar to *PLCδ1*, we generated mice lacking both *PLCδ1* and *PLCδ3* genes (*PLCδ1*/*PLCδ3* double-knockout [DKO] mice). We found that simultaneous disruption of *PLCδ1* and *PLCδ3* resulted in embryonic lethality at midgestation. In *PLCδ1*/*PLCδ3* DKO mice, the structure of the placental labyrinth layer was abnormal, and placental vascularization was decreased. Furthermore, tetraploid (4N) aggregation experiments revealed that the primary cause of embryonic lethality is a trophoblast defect. Thus, PLCδ1 and PLCδ3 play important roles in normal development of the placenta.

* Corresponding author. Mailing address: Laboratory of Genome and Biosignal, Tokyo University of Pharmacy and Life Science, 1432-1 Horinouchi, Hachioji, 192-0392 Tokyo, Japan. Phone: 81-426-76-7214. Fax: 81-426-76-7249. E-mail: kfukami@ls.toyaku.ac.jp.

MATERIALS AND METHODS

Generation of *PLCδ3* KO mice. *PLCδ3* heterozygous (*PLCδ3*$^{+/-}$) mice were generated by Lexicon Genetics Incorporated (The Woodlands, TX) from Omni Bank clone OST101546 as described previously (37). Once germ line transmission had been validated by PCR, the *PLCδ3*$^{+/-}$ animals were mated with an animal with a C57BL/6J background, resulting in a 129Sv/lex × C57BL/6J hybrid background.

Mouse breeding to generate *PLCδ1*/*PLCδ3* DKO mice. *PLCδ1* KO strains have been described previously (18). To generate *PLCδ1*/*PLCδ3* DKO mice, the *PLCδ1* and *PLCδ3* KO mouse lines were interbred. Mouse tail tips, small parts of yolk sacs, or embryos were used for genotyping by PCR. Primers for PCR analysis of PLCδ1 were described previously (18). Primers for PLCδ3 were 5′-TTAACCTGATGCTCCTGAGG-3′, 5′-GGATAAAATGCTTGCCCTGC-3′, and 5′-AAAATGGCGTTACTTAAGCTTGC-3′. Gene targeting was also verified by Western blot analysis with appropriate antibodies.

Antibodies and Western blot analysis. Mouse monoclonal antibodies against PLCδ3 were developed by immunizing *PLCδ3* KO mice with full-length mouse PLCδ3 protein as an antigen. PLCδ1 polyclonal antibody was a gift from Pann-Ghill Suh (POSTECH, Korea). Anti-β-actin antibody was purchased from Chemicon (Temecula, CA). Various tissues or cells for Western blot analysis were homogenized with a buffer (50 mM Tris-HCl, pH 7.5, 150 mM NaCl, 2 mM EDTA, 1% Triton X-100), sonicated, and centrifuged for 15 min at 13,000 × *g* to remove insoluble debris. Sodium dodecyl sulfate (SDS) sample buffer was then added, and the mixture was incubated for 5 min at 95°C. The lysates were resolved by SDS-polyacrylamide gel electrophoresis, transferred to nitrocellulose membranes, and probed with antibodies as described previously (17).

Histochemistry and immunohistochemistry. For histological analyses, placentas were fixed in 4% paraformaldehyde or 2% glutaraldehyde, dehydrated, and embedded in paraffin. Sections (5 μm) were stained with hematoxylin and eosin (HE). For PLCδ1 immunohistochemistry, placentas were fixed overnight in 4% paraformaldehyde at 4°C and embedded in paraffin. Paraffin sections (5 μm) were prepared. These sections were boiled in a microwave oven in 10 mM sodium citrate buffer (pH 6.0) for antigen retrieval and incubated with rabbit polyclonal anti-PLCδ1 antibody, followed by the procedure described in the technical bulletin of the tyramide signal amplification immunodetection kit (Perkin-Elmer, Boston, MA). Whole-mount CD31 staining of embryonal heads and yolk sacs was performed as described previously (36).

TUNEL assay and BrdU labeling. Terminal deoxynucleotidyl transferase-mediated dUTP-biotin nick end labeling (TUNEL) assays were performed with an ApopTag Plus Peroxidase *In Situ* Apoptosis Detection Kit (CHEMICON) according to the manufacturer's recommendations. bromodeoxyuridine (BrdU) labeling was performed with a 5-Bromo-2′-Deoxyuridine Labeling and Detection Kit II (Roche Diagnostics, Mannheim, Germany) according to the manufacturer's recommendations by intraperitoneal injection of BrdU into pregnant mice.

Electron microscopy. Placentas were fixed with 3% glutaraldehyde in 0.1 M phosphate buffer (pH 7.3). Specimens were postfixed with 2% osmium tetroxide for 2 h, block stained with 3% uranyl acetate for 2 h, and embedded in epoxy resin. Thin sections were cut, stained with uranyl acetate and lead citrate, and examined with a Hitachi H-800 transmission electron microscope.

Tetraploid chimera experiment. Two-cell-stage embryos were obtained from the oviducts of B6C3F1 females at embryonic day 1.5 (E1.5). The two-cell-stage embryos were placed in 0.3 M mannitol and aligned in a 5-V AC field and fused with two 40-μs 150-V DC pulses from a 1-mm electrode and a BTX Electro Cell Manipulator 2001 electrofusion apparatus (BTX, San Diego, CA). Fused embryos were cultured overnight. The zona was removed, and four- or eight-cell-stage diploid (2N) embryos derived from *PLCδ1*$^{-/-}$ *PLCδ3*$^{+/-}$ intercross matings were aggregated with four-cell-stage 4N B6C3F1 embryos. Chimeric embryos that developed successfully into blastocysts were transferred to the uterus of a pseudopregnant female.

RESULTS

Generation of *PLCδ3* KO and *PLCδ1*/*PLCδ3* DKO mice. To date, KO mice for many PLC isozymes have been generated and analyzed (5). Interestingly, these KO mice displayed distinct phenotypes, suggesting that although there are as many as 13 PLC isozymes, each has unique physiological functions. Therefore, we attempted to elucidate the physiological functions of PLCδ3 by generating and analyzing *PLCδ3* KO mice. We first searched the Omni Bank embryonic stem (ES) cell library (Lexicon Genetics Incorporated) and identified one ES cell clone (OST101546) that had a retroviral gene trap insertion between exon 1, which contains the translation initiation codon, and exon 2 of the *PLCδ3* mRNA. ES cell clone OST101546 was used to generate the *PLCδ3* KO mice (Fig. 1A). Disruption of *PLCδ3* was confirmed by PCR analysis of genomic DNA (Fig. 1B) and Western blot analysis of protein from the heart (Fig. 1C). *PLCδ3* KO mice were viable, fertile, and apparently normal (Fig. 1D). Western blot analysis revealed that the tissue distribution of PLCδ3 overlaps that of PLCδ1 (Fig. 1E), which shares high homology with *PLCδ3* (Fig. 1F), suggesting that the two genes may be functionally redundant. To investigate this possibility, we next generated *PLCδ1*/*PLCδ3* DKO mice (Fig. 1G). *PLCδ1*$^{-/-}$ *PLCδ3*$^{+/-}$ and *PLCδ1*$^{+/-}$ *PLCδ3*$^{-/-}$ mice appeared normal; however, progressive hair loss, which is the characteristic phenotype of *PLCδ1* KO mice, was observed in the *PLCδ1*$^{-/-}$ *PLCδ3*$^{+/-}$ mice. Intercrosses of *PLCδ1*$^{-/-}$ *PLCδ3*$^{+/-}$ mice produced no *PLCδ1*/*PLCδ3* DKO pups, indicating that double disruption of *PLCδ1* and *PLCδ3* results in embryonic lethality.

To determine the time of embryonic lethality, embryos at various stages of gestation were isolated. By E10.5, *PLCδ1*/*PLCδ3* DKO embryos were detected at the expected Mendelian frequency (Table 1) and were indistinguishable from *PLCδ1*$^{-/-}$ *PLCδ3*$^{+/+}$ littermates. However, by E11.5, 43% of *PLCδ1*/*PLCδ3* DKO embryos were dead or abnormal, and the proportion of dead or abnormal embryos had increased to 56% by E12.5. By E13.5, all *PLCδ1*/*PLCδ3* DKO embryos were dead or visibly abnormal. At E11.5, most living *PLCδ1*/*PLCδ3* DKO embryos appeared normal (Fig. 2A and B), but the hearts of some *PLCδ1*/*PLCδ3* DKO embryos had stopped beating. At E12.5, the body sizes of *PLCδ1*/*PLCδ3* DKO embryos were smaller than those of *PLCδ1*$^{-/-}$ *PLCδ3*$^{+/+}$ embryos, and hemorrhages in the cardiac and ventral body wall regions were visible in some *PLCδ1*/*PLCδ3* DKO embryos (Fig. 2D). In addition, the yolk sacs of *PLCδ1*/*PLCδ3* DKO mice appeared pale, with few vessels and blood cells (Fig. 2E and F). These observations indicate that PLCδ1 and PLCδ3 are required for normal embryonic development.

Vascular defects in *PLCδ1*/*PLCδ3* DKO embryos. The vascular system undergoes significant development during midgestation, which is the time when *PLCδ1*/*PLCδ3* DKO embryos die. Therefore, we investigated the development of the vascular system in *PLCδ1*/*PLCδ3* DKO embryos. Development of the embryonic vascular system involves two distinct processes: vasculogenesis and angiogenesis. During vasculogenesis, angioblasts are committed to an endothelial cell fate and form the primitive vascular plexus. The endothelial cells in the primitive vascular plexus then proliferate, migrate, and form complex vascular networks that contain vessels with various diameters and many branches in a process known as angiogenesis. In *PLCδ1*/*PLCδ3* DKO embryos, vasculogenesis occurred normally (data not shown); however, some defects in angiogenesis were observed. At E12.5, vascular remodeling into small and large vessels had occurred in the head region of *PLCδ1*$^{-/-}$ *PLCδ3*$^{+/+}$ embryos (Fig. 2G), whereas large-diameter vessels, which appeared to be irregularly shaped, were observed in the head region of *PLCδ1*/*PLCδ3* DKO embryos (Fig. 2H). In addition, yolk sacs of E12.5 *PLCδ1*$^{-/-}$ *PLCδ3*$^{+/+}$ embryos contained a complex vascular network that was composed of

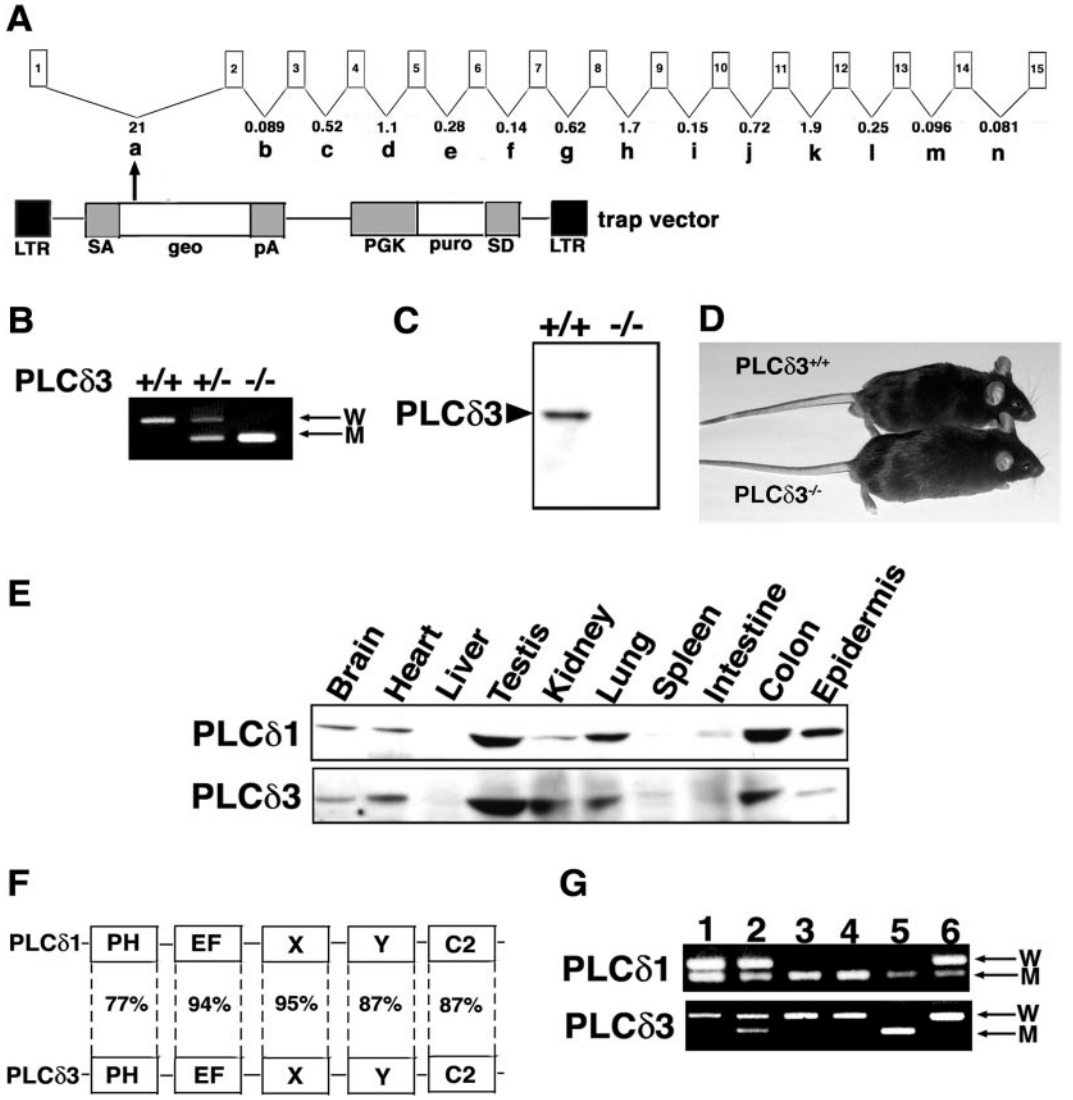

FIG. 1. Generation of *PLCδ3* KO and *PLCδ1*/*PLCδ3* DKO mice. (A) Genetic map of the genomic structure of the *PLCδ3* gene. Exons are indicated by numbered boxes. Introns are lettered (a through n), and their approximate lengths in kbp are given. The structure of the retroviral trap vector to disrupt the mouse *PLCδ3* is also shown. LTR, long terminal repeat; SA, splice acceptor site; geo, galactosidase-neomycin resistance fusion gene; pA, polyadenylation consensus site; PGK, PGK promoter; puro, puromycin resistance cassette; SD, splice donor site. The gene trap is inserted into intron a of the *PLCδ3* gene as indicated by an arrow. (B) PCR genotyping. Genomic DNAs were isolated from tails of wild-type (+/+), heterozygous (+/−), and *PLCδ3* KO (−/−) mice. W, wild type; M, mutant. (C) Western blot analysis of expression of PLCδ3 in heart from wild-type (+/+) and *PLCδ3* KO (−/−) mice. (D) Dorsal view of $PLC\delta3^{+/+}$ and $PLC\delta3^{-/-}$ mice. (E) Western blot analysis of the tissue distribution of PLCδ1 and PLCδ3. Protein (40 μg) was subjected to SDS-polyacrylamide gel electrophoresis, and Western blot analysis was performed. (F) Amino acid homology between PLCδ1 and PLCδ3. Numbers indicate the percentage of similar amino acids. PH, pleckstrin homology domain; EF, EF-hand motif; X, X domain; Y, Y domain; C2, C2 domain. (G) Genotyping of embryos from $PLC\delta1^{+/-}$ $PLC\delta3^{+/-}$ intercrosses at E11.5. Lane 5, *PLCδ1*/*PLCδ3* DKO embryos. W, wild type; M, mutant.

large- and small-diameter vessels (Fig. 2I), whereas yolk sacs from *PLCδ1*/*PLCδ3* DKO embryos contained a relatively simple vascular network that consisted of equal-diameter vessels (Fig. 2J).

Thus, angiogenic remodeling did not occur normally in *PLCδ1*/*PLCδ3* DKO embryos. However, these vascular defects were observed only in embryos that were obviously abnormal or already dead. Therefore, we speculated that there was another defect that contributed to embryonic lethality in *PLCδ1*/*PLCδ3* DKO embryos.

Abundant expression of PLCδ1 and PLCδ3 in placenta. Around E11.5 to E13.5, placental defects are one of the main causes of embryonic lethality. Therefore, we examined expression of PLCδ1 and PLCδ3 in various tissues, including the placenta. Western blotting of tissues from E11.5 embryos revealed that both PLCδ1 and PLCδ3 exist most abundantly in the placenta (Fig. 3A). We confirmed that PLCδ1 levels were comparable between maternal decidual tissue and the embryonic origin of the placenta, whereas PLCδ3 was expressed more abundantly in the maternal part, but a significant level of

TABLE 1. Genotypes of offspring from *PLCδ1*$^{-/-}$ *PLCδ3*$^{+/-}$ × *PLCδ1*$^{-/-}$ *PLCδ3*$^{+/-}$ mating

Day of analysis	No. with genotype[a]:			Total
	δ1$^{-/-}$ *δ3*$^{+/+}$	*δ1*$^{-/-}$ *δ3*$^{+/-}$	*δ1*$^{-/-}$ *δ3*$^{-/-}$	
E9.5	16	24	8	48
E10.5	14	34	23	71
E11.5	56	121	51 (22)	228
E12.5	38	73	32 (18)	143
E13.5	20	30	17 (17)	67
P0[b]	12	21	0	33

[a] Numbers of dead or abnormal embryos are indicated in parentheses.
[b] P0, postnatal day 0.

PLCδ3 protein was still detected in the embryonic part (Fig. 3B). The embryonic portion of the placenta is composed mainly of trophoblasts. Therefore, we examined the expression of PLCδ1 and PLCδ3 in trophoblast stem (TS) cells, which differentiate into giant trophoblasts by depleting culture medium of fibroblast growth factor (30). PLCδ1 and PLCδ3 levels in lysates of TS cells were significantly higher than those of mouse embryonic fibroblasts, although the levels of PLCδ1 and PLCδ3 did not change during differentiation of TS cells (Fig. 3C). Furthermore, we carried out immunohistochemical analysis. Immunohistochemical analysis with anti-PLCδ1 antibody showed that PLCδ1 was expressed abundantly in trophoblasts of wild-type placentas (Fig. 3D and F), although PLCδ3 expression could not be detected because of the unavailability of our anti-PLCδ3 antibody for immunohistochemical analysis (data not shown). We also confirmed that PLCδ1 immunoreactivity was not detected in placentas of *PLCδ1* KO mice (Fig. 3E), indicating that the signal is specific. These data indicate that PLCδ1 and PLCδ3 are expressed at high levels in trophoblasts of the placenta.

Reduced vascularization of the labyrinth area in *PLCδ1*/*PLCδ3* DKO placenta. Because PLCδ1 and PLCδ3 are expressed at high levels in the placenta, we analyzed morphological changes in placentas from *PLCδ1*$^{-/-}$ *PLCδ3*$^{+/+}$ and *PLCδ1*/*PLCδ3* DKO embryos by HE staining. The embryonic part of the placenta is composed of three distinct trophoblast cell layers, the labyrinth layer, the spongiotrophoblast layer, and the giant trophoblast layer, moving from the embryo side to the maternal side (28). The labyrinth layer contains a large number of maternal and embryonic vessels and is the site of

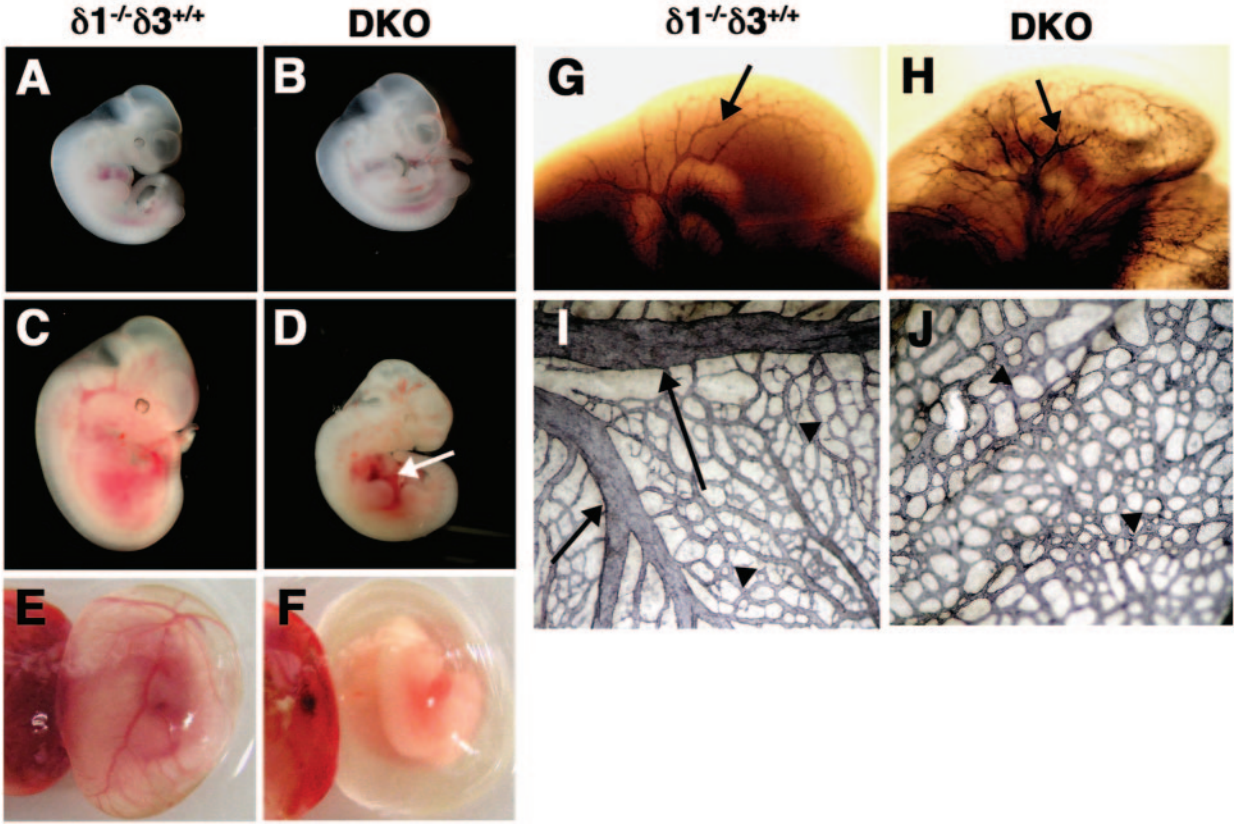

FIG. 2. Macroscopic and vascular abnormalities of *PLCδ1*/*PLCδ3* DKO embryos and extraembryonic tissues. (A to F) Macroscopic views of embryos and yolk sacs. Views of E11.5 *PLCδ1*$^{-/-}$ *PLCδ3*$^{+/+}$ (A) and E11.5 *PLCδ1*/*PLCδ3* DKO (B) embryos and E12.5 *PLCδ1*$^{-/-}$ *PLCδ3*$^{+/+}$ (C) and E12.5 *PLCδ1*/*PLCδ3* DKO (D) embryos. Yolk sacs of E12.5 *PLCδ1*$^{-/-}$ *PLCδ3*$^{+/+}$ (E) and E12.5 *PLCδ1*/*PLCδ3* DKO (F) embryos are also shown. At E12.5, *PLCδ1*/*PLCδ3* DKO embryos exhibit hemorrhaging in the cardiac and ventral body wall regions (arrow in panel D). (G to J) Whole-mount CD31 staining of E12.5 heads and yolk sacs. Vessels of the head regions in *PLCδ1*$^{-/-}$ *PLCδ3*$^{+/+}$ embryos were well remodeled (arrow in panel G), whereas in *PLCδ1*/*PLCδ3* DKO embryos, the vasculature of the head region was irregularly shaped (arrow in panel H). Yolk sac vessels of *PLCδ1*$^{-/-}$ *PLCδ3*$^{+/+}$ embryos were well remodeled with both large (arrows in panel I) and small (arrowheads in panel I) vessels, whereas those of *PLCδ1*/*PLCδ3* DKO embryos contained mostly equal-diameter vessels (arrowheads in panel J).

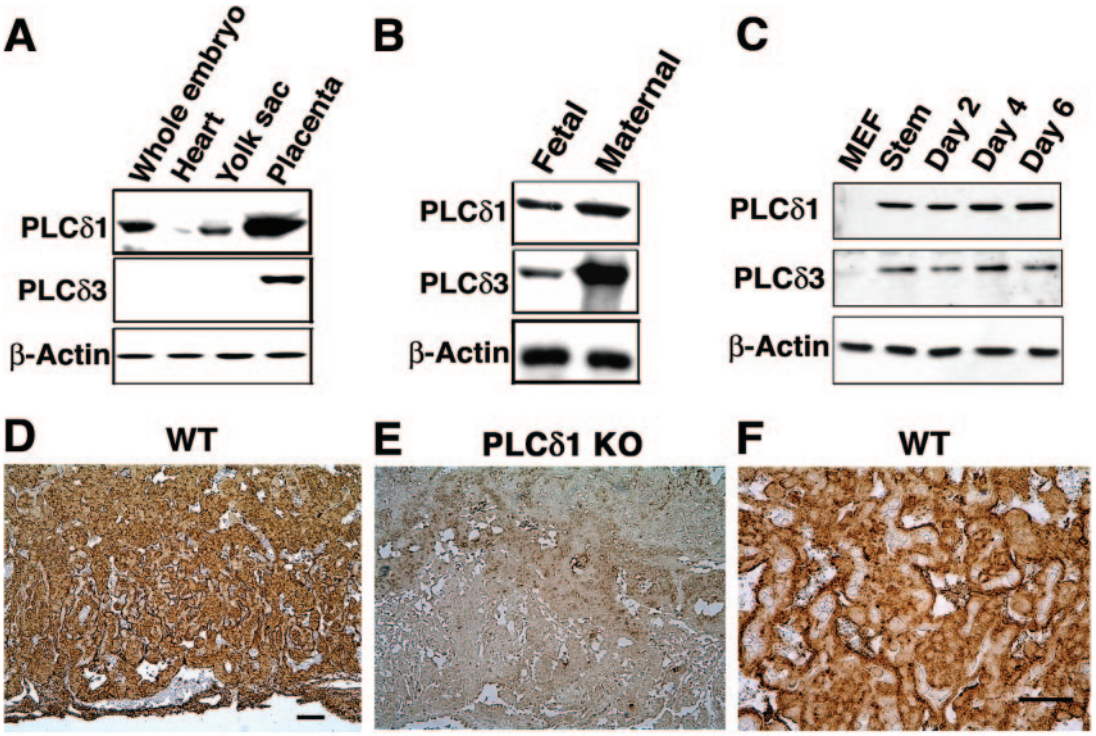

FIG. 3. Expression of PLCδ1 and PLCδ3 in placenta and trophoblast. (A) Western blot analysis of expression of PLCδ1 and PLCδ3 in embryonic and extraembryonic tissues at E11.5. (B) Western blot analysis of expression of PLCδ1 and PLCδ3 in fetal and maternal parts of the placenta. (C) PLCδ1 and PLCδ3 are expressed at high levels in TS cells. MEF, mouse embryonic fibroblast; Stem, undifferentiated TS cells; Day 2, Day 4, and Day 6, TS cells were induced to differentiate for 2 days, 4 days, and 6 days, respectively. β-Actin (A to C) was included as a loading control. (D to F) Immunohistochemical detection of PLCδ1 in the placenta. Immunohistochemical staining of wild-type (D and F) and *PLCδ1* KO (E) placentas at E11.5 with a polyclonal anti-PLCδ1 antibody. (F) Magnified view of panel D. Bars: D and E (shown in panel D) = 100 μm; F = 50 μm.

oxygen, nutrient, and waste exchange between the mother and the embryo. At E10.5, the structures of the labyrinth layers in *PLCδ1*$^{-/-}$ *PLCδ3*$^{+/+}$ and *PLCδ1*/*PLCδ3* DKO placentas were indistinguishable. The numbers of embryonic and maternal vessels were also similar (Fig. 4A to D). At this stage, embryonic vessels (Fig. 4C and D) in the labyrinth area could be discriminated from maternal vessels (Fig. 4C and D) on the basis of differences in hemocyte morphology. However, at E11.5, we observed a remarkable difference in the labyrinth structure between *PLCδ1*$^{-/-}$ *PLCδ3*$^{+/+}$ and *PLCδ1*/*PLCδ3* DKO placentas. The labyrinth layer of *PLCδ1*$^{-/-}$ *PLCδ3* $^{+/+}$ placentas contained many maternal and embryonic vessels (Fig. 4E and G), whereas the numbers of these vessels in the labyrinth layer of *PLCδ1*/*PLCδ3* DKO placentas were severely reduced (Fig. 4F and H). We also noticed that the labyrinth layer of *PLCδ1*$^{-/-}$ *PLCδ3*$^{+/+}$ placentas was reddish, whereas the color of *PLCδ1*/*PLCδ3* DKO placentas was somewhat yellowish (data not shown), suggesting reduced vascularization. These abnormalities were already observed in apparently normal *PLCδ1*/*PLCδ3* DKO embryos at E11.5. When we calculated the ratio of the vascularized area to the total labyrinth area using NIH Image software, the ratio in *PLCδ1*/*PLCδ3* DKO placentas was much lower (0.15 ± 0.038) than that in *PLCδ1*$^{-/-}$ *PLCδ3*$^{+/+}$ placentas (0.27 ± 0.035) (Fig. 4I). The ratios of the vascularized area to the total labyrinth area were comparable in *PLCδ1*$^{-/-}$ *PLCδ3*$^{+/+}$ and *PLCδ1*/*PLCδ3* DKO placentas at E10.5, suggesting that the abnormal morphological changes in the *PLCδ1*/*PLCδ3* DKO placenta occur between E10.5 and E11.5. These abnormalities lead to insufficient exchange of gas, nutrients, and waste and therefore are likely to cause the midgestational embryonic lethality of *PLCδ1*/*PLCδ3* DKO mice.

Reduced proliferation and aberrant apoptosis in cells of *PLCδ1*/*PLCδ3* DKO labyrinth area. The developmental defect in the labyrinth area of *PLCδ1*/*PLCδ3* DKO mice suggests that proliferation of cells in this area is abnormal. Therefore, we examined the proliferative activity of cells in the labyrinth layer using BrdU incorporation. At E11.5, the *PLCδ1*$^{-/-}$ *PLCδ3*$^{+/+}$ labyrinth layer contained many BrdU-positive cells (Fig. 5A and C). In contrast, the *PLCδ1*/*PLCδ3* DKO labyrinth area displayed low BrdU incorporation (Fig. 5B and D). We also found that the labyrinth layer of the *PLCδ1*/*PLCδ3* DKO placenta contained necrotic or apoptotic cells (Fig. 5E). Therefore, we next analyzed apoptosis in sections of the placenta using the TUNEL technique. Few or no TUNEL-positive cells were observed in the labyrinth layer of *PLCδ1*$^{-/-}$ *PLCδ3*$^{+/+}$ placentas (Fig. 5F), whereas many TUNEL-positive cells were present in the labyrinth layer of *PLCδ1*/*PLCδ3* DKO placentas (Fig. 5G and H). The necrotic or apoptotic cells exhibited an elongated morphology and were similar to syncytiotrophoblasts, which are located between a layer of mononuclear trophoblasts that line the maternal sinusoids and fetal endothelial

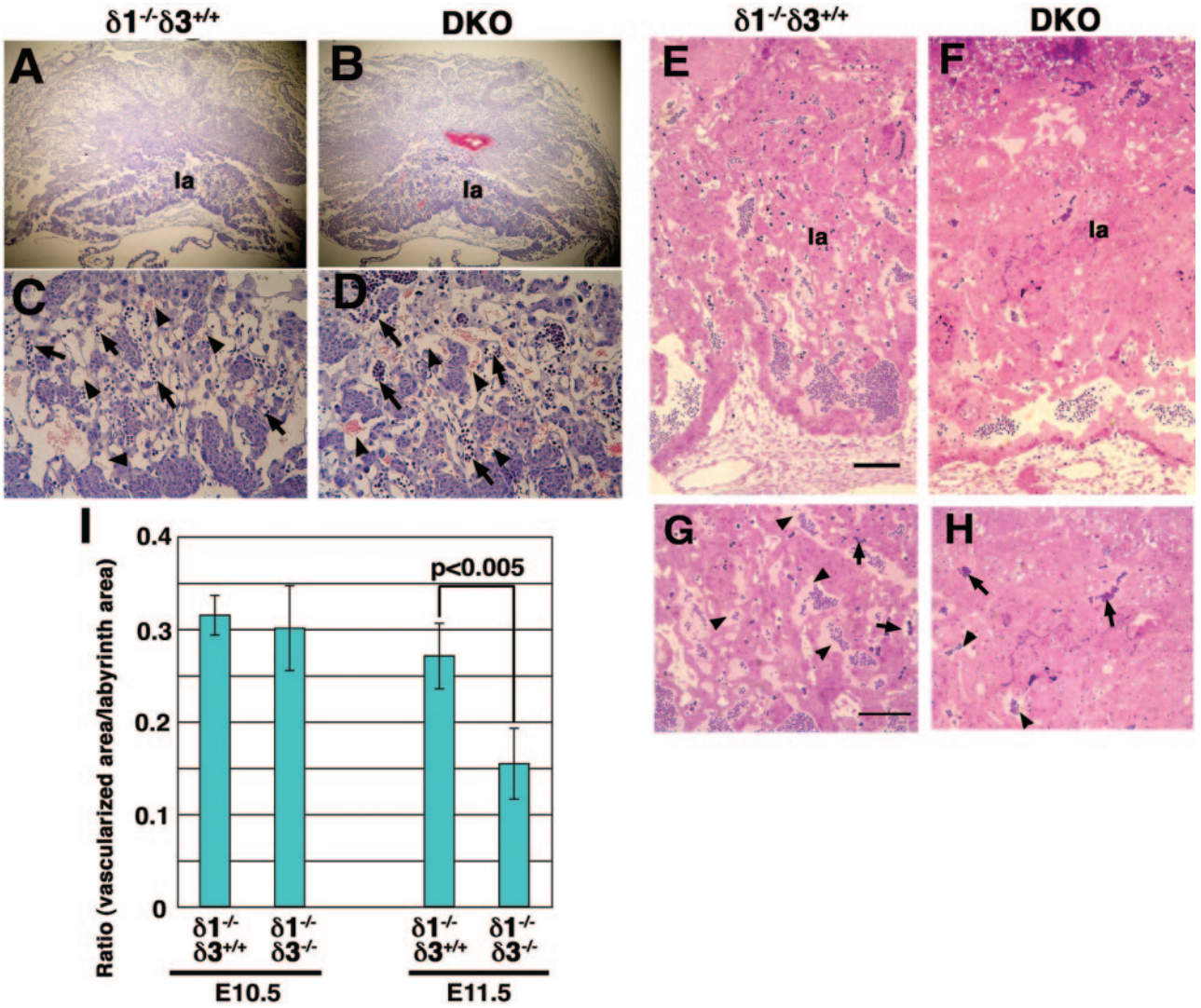

FIG. 4. Histological abnormalities in placentas of *PLCδ1/PLCδ3* DKO mice. (A to H) HE staining of placenta sections from *PLCδ1*$^{-/-}$ *PLCδ3*$^{+/+}$ (A, C, E, and G) and *PLCδ1/PLCδ3* DKO (B, D, F, and H) embryos at E10.5 (A to D) and E11.5 (E to H). The arrows indicate embryonal vessels, and the arrowheads indicate maternal vessels. la, labyrinth area. Note that vascularization is reduced in the labyrinth area of the *PLCδ1/PLCδ3* DKO placenta (F and H). (I) For quantification, the ratio of the vascularized area to the total labyrinth area was calculated with NIH Image software. Values represent the average ratios in five fields from five sections from different mice. Statistical significance was determined by Student's *t* test; the error bars indicate standard deviations. Bars: E and F (shown in panel E) = 100 μm; G and H (shown in panel G) = 50 μm.

cells and play a critical role in nutrient transport (28). We then performed ultrastructural analysis of cells in the labyrinth layer of *PLCδ1/PLCδ3* DKO mice to identify dead cells and confirm the presence of features associated with apoptosis. In the *PLCδ1*$^{-/-}$ *PLCδ3*$^{+/+}$ placenta, we observed endothelial cells, syncytiotrophoblasts, and mononucleated trophoblasts, which have intact cellular structure, between the embryonic vessels and maternal vessels (Fig. 5I). In contrast, vacuolation of nuclei (Fig. 5J, K, L, and M) and trophoblast fragmentation (Fig. 5J, K, N, O, and P) were observed in the labyrinth area of *PLCδ1/PLCδ3* DKO placentas. Such trophoblast fragmentation and nuclear vacuolation were never observed in *PLCδ1*$^{-/-}$ *PLCδ3*$^{+/+}$ placentas (Fig. 5I). In addition, endothelial cells of *PLCδ1/PLCδ3* DKO placentas appeared normal even when the surrounding trophoblasts had died (Fig. 5J, K, O, and P), indicating that apoptosis of *PLCδ1/PLCδ3* DKO trophoblasts is a primary phenomenon. Furthermore, electron microscopy revealed that the dead cells were positioned mainly just outside of embryonic endothelial cells (Fig. 5J, K, O, and P), indicating that the dead cells in *PLCδ1/PLCδ3* DKO placentas were syncytiotrophoblasts. These results were consistent with those of HE (Fig. 5E) and TUNEL staining (Fig. 5H) and suggest that PLCδ1 and PLCδ3 influence the survival and proliferation of trophoblasts in the labyrinth layer of the placenta.

Rescue of *PLCδ1/PLCδ3* DKO embryos from embryonic lethality by supplying wild-type placenta. Because *PLCδ1/PLCδ3* DKO embryos show vascular defects (Fig. 2G to J), as well as placental trophoblast defects, we attempted to examine whether the primary cause of embryonic lethality of *PLCδ1/PLCδ3* DKO mice is the placental trophoblast defect. We

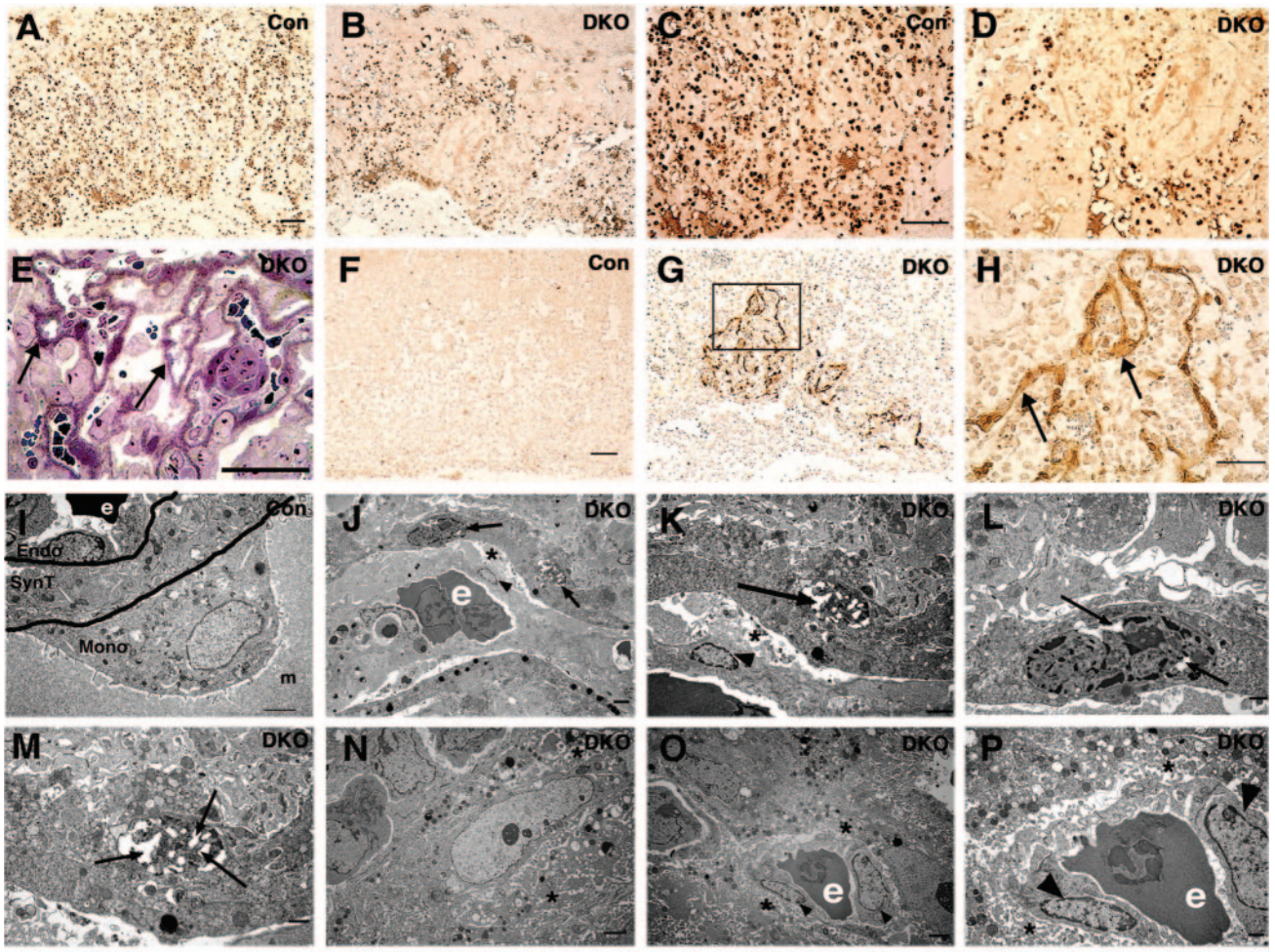

FIG. 5. Apoptotic and proliferative defects in trophoblasts of *PLCδ1*/*PLCδ3* DKO placenta. (A to D) Proliferative activity was determined by BrdU incorporation analysis of labyrinth layer cells in *PLCδ1*$^{-/-}$ *PLCδ3*$^{+/+}$ (A and C) and *PLCδ1*/*PLCδ3* DKO (B and D) placentas. (C and D) Higher magnifications of the fields in panels A and B, respectively. HE (E) and TUNEL staining (F to H) of *PLCδ1*$^{-/-}$ *PLCδ3*$^{+/+}$ (F) and *PLCδ1*/*PLCδ3* DKO (E, G, and H) placentas. Apoptotic or necrotic cells were observed in the labyrinth area of the *PLCδ1*/*PLCδ3* DKO placenta (arrows in panel E). (H) Higher magnification of the field in panel G. TUNEL-positive cells were observed in the labyrinth area of the *PLCδ1*/*PLCδ3* DKO placenta (arrows in panel H). (I to P) Ultrastructural analysis of cells in *PLCδ1*$^{-/-}$ *PLCδ3*$^{+/+}$ (I) and DKO (J to P) labyrinth layers. Note that the structure composed of mononuclear trophoblast (Mono), syncytiotrophoblast (SynT), and endothelial cell (Endo) is intact in the *PLCδ1*$^{-/-}$ *PLCδ3*$^{+/+}$ labyrinth (I). Arrows (J to M) indicate vacuolation of nuclei in apoptotic trophoblasts. Asterisks (J, K, N, O, and P) indicate fragmented trophoblasts. Arrowheads (J, K, O, and P) indicate endothelial cells. e, embryonic vessels; m, maternal vessels. Bars: A and B (shown in panel A) = 100 μm; C and D (shown in panel C) = 100 μm; E = 50 μm; F and G (shown in panel F) = 100 μm; H = 50 μm; I = 2 μm; J = 2 μm; K = 2 μm; L = 1 μm; M = 1 μm; N = 2 μm; O = 2 μm; P = 1 μm.

aggregated wild-type 4N embryos with 2N embryos derived from *PLCδ1*$^{-/-}$ *PLCδ3*$^{+/-}$ intercrosses. In this case, the wild-type 4N cells contributed exclusively to the placental trophoblast cells and endoderm of the yolk sac, whereas the 2N cells contributed mainly to the embryo proper (12) (Fig. 6A). Thus, if the embryonic lethality of *PLCδ1*/*PLCδ3* DKO mice is due only to a placental trophoblast defect, *PLCδ1*/*PLCδ3* DKO embryos with wild-type placentas should survive beyond E13.5, the time when all *PLCδ1*/*PLCδ3 DKO* embryos were dead or abnormal. With this method, we detected 2 living *PLCδ1*/*PLCδ3* DKO embryos among 16 embryos at E14.5 (Fig. 6B to D). We also examined the morphology of the placentas of *PLCδ1*/*PLCδ3* DKO mice rescued by tetraploid aggregation. In contrast to the labyrinth area of the *PLCδ1*/*PLCδ3* DKO placenta (Fig. 4F and H), the placentas of rescued *PLCδ1*/*PLCδ3* DKO embryos contained many maternal and embryonic vessels, although the ratio of the vascularized area to the total labyrinth area in rescued *PLCδ1*/*PLCδ3* DKO placentas was slightly lower than that of control placentas (Fig. 6E to G). These results clearly indicate that the embryonic lethality observed in *PLCδ1*/*PLCδ3* DKO mice is caused primarily and mainly by trophoblast defects.

DISCUSSION

In the present study, we attempted to elucidate the physiological functions of PLCδ3 by analyzing *PLCδ3* KO mice (Fig. 1A to C). *PLCδ3* KO mice appeared normal (Fig. 1D); however, we cannot rule out the possibility that functional abnormalities are present in some organs or systems of *PLCδ3* KO mice. PLCδ3

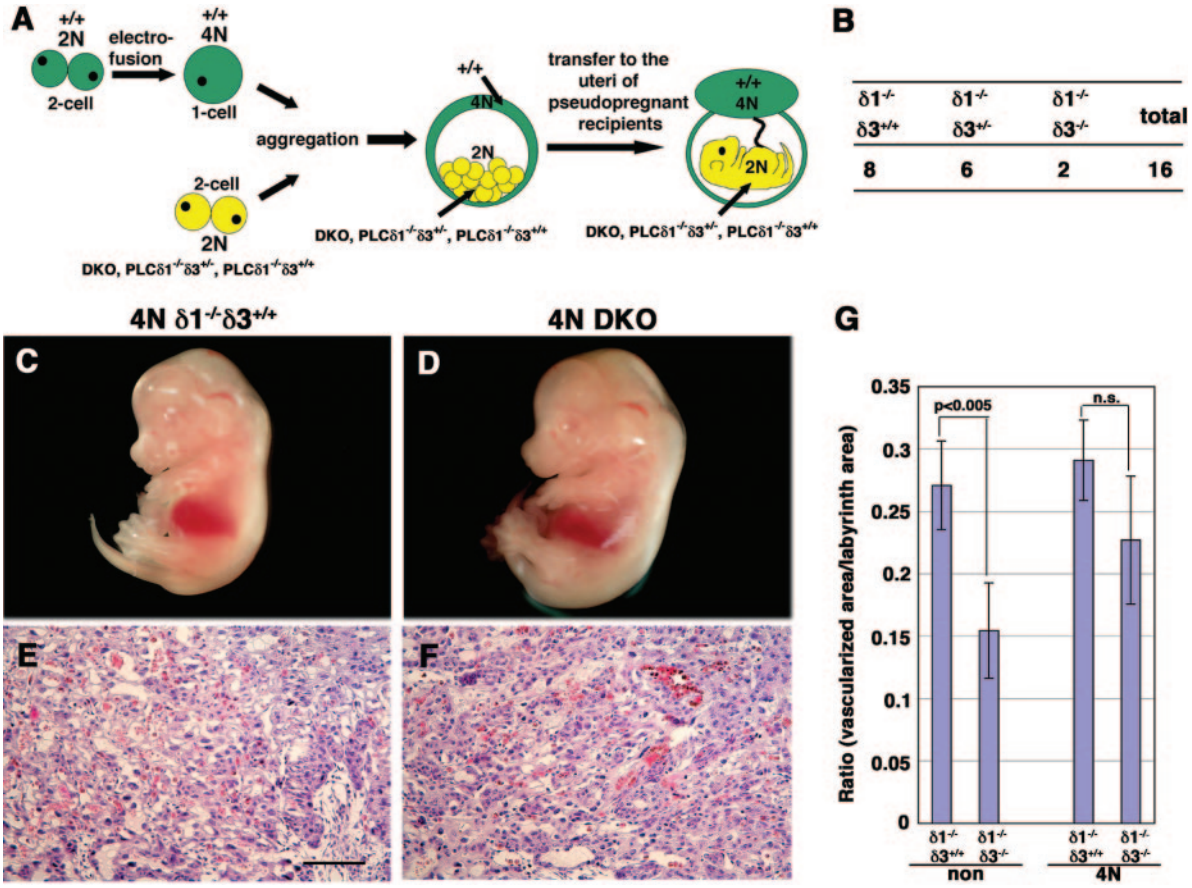

FIG. 6. Rescue of *PLCδ1/PLCδ3* DKO placenta and embryo by tetraploid aggregation method. (A) Strategy of tetraploid chimera generation. 4N wild-type cells (+/+) were generated by electrofusion of 2N wild-type cells, and then 4N wild-type cells and 2N cells from intercrosses between *PLCδ1*$^{-/-}$ *PLCδ3*$^{+/-}$ (DKO; *δ1*$^{-/-}$ *δ3*$^{+/-}$ and *δ1*$^{-/-}$ *δ3*$^{+/+}$) were aggregated. Blastocysts resulting from the aggregations were transferred into the uteri of pseudopregnant recipient mice. (B) Number of embryos generated by 4N aggregation method at E14.5. Aggregation of 4N wild-type cells and 2N cells from *PLCδ1*$^{-/-}$ *PLCδ3*$^{+/-}$ intercrosses was carried out. (C and D) Macroscopic views of rescued *PLCδ1*$^{-/-}$ *PLCδ3*$^{+/+}$ (C) and *PLCδ1/PLCδ3* DKO (D) embryos at E14.5. No obvious abnormalities were observed in the rescued *PLCδ1/PLCδ3* DKO embryos. (E and F) HE staining of sections of placentas from rescued *PLCδ1*$^{-/-}$ *PLCδ3*$^{+/+}$ (E) and *PLCδ1/PLCδ3* DKO (F) embryos at E14.5. (G) Quantification of the ratio of vascularized area to total labyrinth area in nonrescued or 4N aggregation-rescued placenta. The values represent the average ratios in four fields from two sections from different tetraploid rescued mice (4N) and in five fields from five sections from different nonrescued mice (non). Statistical significance was determined by Student's *t* test. n.s., not significant. The error bars represent standard deviations.

has the highest sequence homology to PLCδ1, and the proteins have similar tissue distribution patterns (Fig. 1E and F). In addition, *PLCδ1* KO mice showed no obvious abnormalities, except for disturbance of skin homeostasis and runting (18). These facts suggest that PLCδ1 and PLCδ3 are functionally redundant and that the phenotypes were masked in single-gene KO mice. Therefore, we generated PLCδ1/δ3 DKO mice and found that these mice died in midgestation (Table 1).

The primary cause of embryonic lethality was defective development of the placenta. The placenta is composed of the maternal decidual tissue and a fetal portion that consists of three distinct trophoblast cell layers. Among these layers, the labyrinth layer contains many maternal and fetal vessels and plays a critical role in the exchange of nutrients and gas between the mother and the embryo. Therefore, normal placental function is essential for development of the embryo. We found that the labyrinth layer of *PLCδ1/PLCδ3* DKO placentas contains fewer maternal and embryonic vessels (Fig. 4F and H). In addition, trophoblasts of the labyrinth layer of *PLCδ1/PLCδ3* DKO placentas displayed aberrant cell death (Fig. 5E, G, and H). Cell death of some endothelial cells was also observed. However, electron microscopy revealed that trophoblasts died earlier than endothelial cells (Fig. 5J, K, O, and P). Therefore, a trophoblast abnormality was the primary cause of aberrant cell death and reduced proliferation of cells (Fig. 5B and D) in the placental labyrinth area, and death of endothelial cells may be a secondary effect of the death of surrounding trophoblasts. Because trophoblasts secrete several angiogenic factors, which play important roles in the growth and survival of endothelial cells and trophoblasts (38), it is possible that *PLCδ1/PLCδ3* DKO trophoblasts secret insufficient angiogenic factors, which leads to reduced vascularization in *PLCδ1/PLCδ3* DKO placentas. Therefore, we examined the expression levels of angiogenic factors, such as vascular endothelial growth factor (VEGF), placenta growth factor (PlGF), angiopoietin 1, and angiopoietin 2 in E11.5 *PLCδ1*$^{-/-}$ *PLCδ3*$^{+/+}$ and *PLCδ1/PLCδ3* DKO placentas by reverse transcription-PCR analysis and found that there were no significant differ-

ences in the expression levels of these genes between *PLCδ1*$^{-/-}$ *PLCδ3*$^{+/+}$ and *PLCδ1*/*PLCδ3* DKO placentas (data not shown). We also found that the labyrinth structures were normal and that many fetal and maternal vessels were present in *PLCδ1*/*PLCδ3* DKO placentas at E10.5 (Fig. 4B and D). This suggests that chorioallantoic fusion and branching occurred normally and that the fetal and maternal vessels in the labyrinth area are formed at this stage. Therefore, PLCδ1 and PLCδ3 may not be essential for morphogenesis of the labyrinth area by E10.5 but may be required for the survival of trophoblasts and maintenance of normal labyrinth structure at later stages.

The labyrinth area contains several distinct subtypes of trophoblasts that are present in specific locations, and these cell types can be readily distinguished on the basis of their positions and morphologies (28, 32). HE staining, TUNEL staining, and electron microscopy revealed that placental defects in *PLCδ1*/*PLCδ3* DKO mice were due mainly to a syncytiotrophoblast abnormality (Fig. 5E, H, K, and O). Syncytiotrophoblast formation is a unique process that involves cell cycle exit and then fusion of these cells to form a syncytium (28). However, very little is known about the mechanism that underlies fusion of mouse trophoblasts. We investigated the expression levels of syncytins, which was reported to play the critical role in syncytiotrophoblast formation (2, 16), in E11.5 *PLCδ1*$^{-/-}$ *PLCδ3*$^{+/+}$ and *PLCδ1*/*PLCδ3* DKO placentas by reverse transcription-PCR analysis and found that there were no remarkable differences in the expression levels of syncytin between *PLCδ1*$^{-/-}$ *PLCδ3*$^{+/+}$ and *PLCδ1*/*PLCδ3* DKO placentas (data not shown). Syncytiotrophoblasts play critical roles in normal placental function and embryo development. Exchange of nutrients and waste in the labyrinth area is dependent on syncytiotrophoblast functions, including endocytosis, exocytosis, and transcytosis (4). Phosphoinositide metabolism has been reported to be involved in membrane fusion or trafficking events, such as clathrin-mediated internalization of receptors or exocytosis of neurotransmitters (11, 33). Therefore, phosphoinositide metabolism may play important roles in the formation and function of syncytiotrophoblasts, and disturbance of phosphoinositide metabolism by deletion of the *PLCδ1* and *PLCδ3* genes may lead to syncytiotrophoblast abnormalities.

Because some dead or abnormal *PLCδ1*/*PLCδ3* DKO embryos show vascular defects (Fig. 2G to J) in addition to placental defects, we used the tetraploid aggregation technique (Fig. 6A) to clarify placental trophoblast defects. The embryonic lethality by E13.5 was rescued by this method (Fig. 6B to F), indicating clearly that trophoblast abnormalities cause lethality of *PLCδ1*/*PLCδ3* DKO embryos at this stage. However, the defect in vascularization of the labyrinth area of rescued *PLCδ1*/*PLCδ3* DKO mice was not completely rescued, although a drastic improvement in vascularization was observed (Fig. 6G). It has been reported that wild-type 4N cells contribute exclusively to placental trophoblasts and endoderm of the yolk sac, whereas *PLCδ1*/*PLCδ3* DKO 2N cells contribute to the embryo proper. However, some populations of 2N cells contribute partially to placental trophoblasts, resulting in a placenta that is a chimera of 4N and 2N cells (12). Therefore, the labyrinth area of rescued *PLCδ1*/*PLCδ3* DKO embryos may contain a few 2N *PLCδ1*/*PLCδ3* DKO trophoblasts, and these *PLCδ1*/*PLCδ3* DKO trophoblasts may inhibit complete rescue of vascularization in aggregation experiments.

To date, many genes, including those for transcription factors, growth factors/receptors, and other signal transduction molecules, have been reported to be involved in the development of the placental labyrinth layer (32). However, the molecules upstream and downstream in signaling pathways involving these genes are not fully understood. The results of the present study indicate that PLCδ1 and PLCδ3 must also be considered in placental development. Because PLC activation induces elevation of intracellular calcium levels and protein kinase C activation, leading to modulation of various downstream molecules, it will be very interesting to clarify how PLCδ1 and PLCδ3 affect placental development. One signal transduction pathway that is involved in placental morphogenesis is Rho signaling. It was recently reported that the deleted in liver cancer 1 (*DLC-1*) gene, a Rho GTPase-activating protein, and the rho-associated kinase 2 (*ROCKII*) gene are essential for placental labyrinth layer development (3, 31). Because DLC-1 binds directly to PLCδ1 to activate PLCδ1 enzyme activity (9, 26) and because RhoA inhibits PLCδ1 enzyme activity (8), Rho signaling may modulate PLCδ1 activity during placental development. Together, we show here for the first time that PLCδ1 and PLCδ3 are required for normal morphogenesis and function of the placenta in mice. Although the gross anatomy and physiology of the mouse and human placentas are different, they share considerable cellular and molecular characteristics (25). In addition, intrauterine growth retardation with labyrinth vascular defects has been observed in human preeclampsia and missed abortion (22). Therefore, it is very important to elucidate whether PLCδ1 and PLCδ3 play similar roles in the human placenta, and understanding the signaling pathways that involve PLCδ1 and PLCδ3 may clarify the events in the process of placentogenesis and contribute to the development of treatments for missed abortion and preeclampsia.

ACKNOWLEDGMENTS

We thank Pann-Ghill Suh and Mizuho Sato for PLCδ1 antibodies and technical support, respectively.

This work was supported by a Grant-in-Aid for General Scientific Research from the Japan Ministry of Education, Science, Sports, and Culture and grants from The Naito Foundation and the Uehara Memorial Foundation.

REFERENCES

1. **Berridge, M. J., and R. F. Irvine.** 1984. Inositol trisphosphate, a novel second messenger in cellular signal transduction. Nature **312:**315–321.
2. **Dupressoir, A., G. Marceau, C. Vernochet, L. Benit, C. Kanellopoulos, V. Sapin, and T. Heidmann.** 2005. Syncytin-A and syncytin-B, two fusogenic placenta-specific murine envelope genes of retroviral origin conserved in Muridae. Proc. Natl. Acad. Sci. USA **102:**725–730.
3. **Durkin, M. E., M. R. Avner, C. G. Huh, B. Z. Yuan, S. S. Thorgeirsson, and N. C. Popescu.** 2005. DLC-1, a Rho GTPase-activating protein with tumor suppressor function, is essential for embryonic development. FEBS Lett. **579:**1191–1196.
4. **Fuchs, R., and I. Ellinger.** 2004. Endocytic and transcytotic processes in villous syncytiotrophoblast: role in nutrient transport to the human fetus. Traffic **5:**725–738.
5. **Fukami, K.** 2002. Structure, regulation, and function of phospholipase C isozymes. J. Biochem. (Tokyo) **131:**293–299.
6. **Fukami, K., K. Nakao, T. Inoue, Y. Kataoka, M. Kurokawa, R. A. Fissore, K. Nakamura, M. Katsuki, K. Mikoshiba, N. Yoshida, and T. Takenawa.** 2001. Requirement of phospholipase Cδ4 for the zona pellucida-induced acrosome reaction. Science **292:**920–923.
7. **Fukami, K., M. Yoshida, T. Inoue, M. Kurokawa, R. A. Fissore, N. Yoshida, K. Mikoshiba, and T. Takenawa.** 2003. Phospholipase Cδ4 is required for

Ca2+ mobilization essential for acrosome reaction in sperm. J. Cell Biol. **161:**79–88.
8. **Hodson, E. A., C. C. Ashley, A. D. Hughes, and J. S. Lymn.** 1998. Regulation of phospholipase C-delta by GTP-binding proteins-rhoA as an inhibitory modulator. Biochim. Biophys. Acta **1403:**97–101.
9. **Homma, Y., and Y. Emori.** 1995. A dual functional signal mediator showing RhoGAP and phospholipase C-delta stimulating activities. EMBO J. **14:**286–291.
10. **Irino, Y., H. Cho, Y. Nakamura, M. Nakahara, M. Furutani, P. G. Suh, T. Takenawa, and K. Fukami.** 2004. Phospholipase C δ-type consists of three isozymes: bovine PLCδ2 is a homologue of human/mouse PLCδ4. Biochem. Biophys. Res. Commun. **320:**537–543.
11. **Itoh, T., and T. Takenawa.** 2004. Regulation of endocytosis by phosphatidylinositol 4,5-bisphosphate and ENTH proteins. Curr. Top. Microbiol. Immunol. **282:**31–47.
12. **James, R. M., A. H. Klerkx, M. Keighren, J. H. Flockhart, and J. D. West.** 1995. Restricted distribution of tetraploid cells in mouse tetraploid ↓ diploid chimaeras. Dev. Biol. **167:**213–226.
13. **Katan, M.** 1998. Families of phosphoinositide-specific phospholipase C: structure and function. Biochim. Biophys. Acta **1436:**5–17.
14. **Kato, H., K. Fukami, F. Shibasaki, Y. Homma, and T. Takenawa.** 1992. Enhancement of phospholipase C delta 1 activity in the aortas of spontaneously hypertensive rats. J. Biol. Chem. **267:**6483–6487.
15. **Kelley, G. G., S. E. Reks, J. M. Ondrako, and A. V. Smrcka.** 2001. Phospholipase Cε: a novel Ras effector. EMBO J. **20:**743–754.
16. **Mi, S., X. Lee, X. Li, G. M. Veldman, H. Finnerty, L. Racie, E. LaVallie, X. Y. Tang, P. Edouard, S. Howes, J. C. Keith, Jr., and J. M. McCoy.** 2000. Syncytin is a captive retroviral envelope protein involved in human placental morphogenesis. Nature **403:**785–789.
17. **Nakahara, M., M. Shimozawa, Y. Nakamura, Y. Irino, M. Morita, Y. Kudo, and K. Fukami.** 2005. A novel phospholipase C, PLCη2, is a neuron-specific isozyme. J. Biol. Chem. **280:**29128–29134.
18. **Nakamura, Y., K. Fukami, H. Yu, K. Takenaka, Y. Kataoka, Y. Shirakata, S. Nishikawa, K. Hashimoto, N. Yoshida, and T. Takenawa.** 2003. Phospholipase Cδ1 is required for skin stem cell lineage commitment. EMBO J. **22:**2981–2991.
19. **Nishizuka, Y.** 1988. The molecular heterogeneity of protein kinase C and its implications for cellular regulation. Nature **334:**661–665.
20. **Ochocka, A. M., and T. Pawelczyk.** 2003. Isozymes delta of phosphoinositide-specific phospholipase C and their role in signal transduction in the cell. Acta Biochim. Pol. **50:**1097–1110.
21. **Rebecchi, M. J., and S. N. Pentyala.** 2000. Structure, function, and control of phosphoinositide-specific phospholipase C. Physiol. Rev. **80:**1291–1335.
22. **Regnault, T. R., H. L. Galan, T. A. Parker, and R. V. Anthony.** 2002. Placental development in normal and compromised pregnancies—a review. Placenta **23**(Suppl. A)**:**S119–S129.
23. **Rhee, S. G.** 2001. Regulation of phosphoinositide-specific phospholipase C. Annu. Rev. Biochem. **70:**281–312.
24. **Rhee, S. G., and Y. S. Bae.** 1997. Regulation of phosphoinositide-specific phospholipase C isozymes. J. Biol. Chem. **272:**15045–15048.
25. **Rossant, J., and J. C. Cross.** 2001. Placental development: lessons from mouse mutants. Nat. Rev. Genet. **2:**538–548.
26. **Sekimata, M., Y. Kabuyama, Y. Emori, and Y. Homma.** 1999. Morphological changes and detachment of adherent cells induced by p122, a GTPase-activating protein for Rho. J. Biol. Chem. **274:**17757–17762.
27. **Shimohama, S., Y. Homma, T. Suenaga, S. Fujimoto, T. Taniguchi, W. Araki, Y. Yamaoka, T. Takenawa, and J. Kimura.** 1991. Aberrant accumulation of phospholipase C-delta in Alzheimer brains. Am. J. Pathol. **139:**737–742.
28. **Simmons, D. G., and J. C. Cross.** 2005. Determinants of trophoblast lineage and cell subtype specification in the mouse placenta. Dev. Biol. **284:**12–24.
29. **Song, C., C. D. Hu, M. Masago, K. Kariyai, Y. Yamawaki-Kataoka, M. Shibatohge, D. Wu, T. Satoh, and T. Kataoka.** 2001. Regulation of a novel human phospholipase C, PLCε, through membrane targeting by Ras. J. Biol. Chem. **276:**2752–2757.
30. **Tanaka, S., T. Kunath, A. K. Hadjantonakis, A. Nagy, and J. Rossant.** 1998. Promotion of trophoblast stem cell proliferation by FGF4. Science **282:**2072–2075.
31. **Thumkeo, D., J. Keel, T. Ishizaki, M. Hirose, K. Nonomura, H. Oshima, M. Oshima, M. M. Taketo, and S. Narumiya.** 2003. Targeted disruption of the mouse rho-associated kinase 2 gene results in intrauterine growth retardation and fetal death. Mol. Cell. Biol. **23:**5043–5055.
32. **Watson, E. D., and J. C. Cross.** 2005. Development of structures and transport functions in the mouse placenta. Physiology (Bethesda) **20:**180–193.
33. **Wenk, M. R., and P. De Camilli.** 2004. Protein-lipid interactions and phosphoinositide metabolism in membrane traffic: insights from vesicle recycling in nerve terminals. Proc. Natl. Acad. Sci. USA **101:**8262–8269.
34. **Williams, R. L.** 1999. Mammalian phosphoinositide-specific phospholipase C. Biochim. Biophys. Acta **1441:**255–267.
35. **Yagisawa, H., Y. Emori, and H. Nojima.** 1991. Phospholipase C genes display restriction fragment length polymorphisms between the genomes of normotensive and hypertensive rats. J. Hypertens. **9:**303–307.
36. **Yamazaki, D., S. Suetsugu, H. Miki, Y. Kataoka, S. Nishikawa, T. Fujiwara, N. Yoshida, and T. Takenawa.** 2003. WAVE2 is required for directed cell migration and cardiovascular development. Nature **424:**452–456.
37. **Zambrowicz, B. P., G. A. Friedrich, E. C. Buxton, S. L. Lilleberg, C. Person, and A. T. Sands.** 1998. Disruption and sequence identification of 2,000 genes in mouse embryonic stem cells. Nature **392:**608–611.
38. **Zhou, Y., V. Bellingard, K. T. Feng, M. McMaster, and S. J. Fisher.** 2003. Human cytotrophoblasts promote endothelial survival and vascular remodeling through secretion of Ang2, PlGF, and VEGF-C. Dev. Biol. **263:**114–125.